

4.3 Influence of the Electrical Parameters of the Ignition System on the Phases of Spark Ignition

Tobias Michler, Wooyeong Kim, Olaf Toedter, Thomas Koch, Choongsik Bae

Abstract

With a focus on the spectra of N₂ at 377nm, N₂⁺ at 391nm, N at 500nm and O at 777nm, this paper investigates the influence of additional capacities on the spectrum of spark ignition. For this, an ignition spark with different additional capacities in front of the spark plug was scanned in time. With an increase in capacity, the intensity and duration of an arc discharge, supplied by this capacity, increases strongly. This results in an increase in emissions of nickel in the gas. An increase in the second positive system of nitrogen at 391nm can be observed when the capacity increases. Compared to this the first negative system decreases with increasing capacity. Only during the glow discharge, a strong emission near the cathode was observed. Atomic nitrogen was only observed in the breakdown and capacitive arc modes. With an increase in capacitors the oxygen was reduced.

Kurzfassung

Untersucht wurde der Einfluss der Kapazität auf das Spektrum der Funkenzündung. Im Mittelpunkt der Untersuchung standen die Spektren von N₂ bei 337nm, N₂⁺ bei 391nm, N bei 500nm und O bei 777nm. Dabei wurde ein Zündfunken mit verschiedenen, unmittelbar vor der Zündkerze, montierten Kapazitäten zeitlich abgetastet. Dabei konnte vor allem eine starke Erhöhung der kapazitiv gespeisten Bogenentladung beobachtet werden. Diese resultiert in eine Erhöhung der Nickelemission im Gas. Die 2. pos. Gruppe von Stickstoff bei 337nm weist in dem kapazitiven Bogen eine höhere Intensität auf sobald die Kapazität wächst. Zusätzlich zeigt das Spektrum der 1. neg. Gruppe von Stickstoff bei 391nm erst zum Einsetzen der Glimmentladung eine hohe Leuchterscheinung welche sich auf die Kathode beschränkt. Des Weiteren konnte atomarer Stickstoff nur im Bereich des Durchbruchs und der kapazitiven Bogenentladung gefunden werden. Bei atomarem Sauerstoff konnte eine Reduktion der Emission beobachtet werden.

1 Introduction

The efficiency of SI-engines can be improved significantly by using leaner mixtures [1]. Leaner mixtures cause a reduction of flame velocity and, therefore, a lower heat release at the same input of energy. In order to diminish this effect, prechamber spark plugs could be an opportunity. These spark plugs penetrate the combustion chamber with coils of burning gas. The result is a large area of affected unburned gas which leads to an increase in heat release and an improved combustion.

The problem inherent to the prechamber spark plug is that purging and the involved tail gas reduce the ignition probability related to the air-fuel ratio at the spark plug. To

support the pre chamber spark plug technology, more investigations of the spark plug ignition process and the entire ignition system are required.

The ignition spark will be investigated by examining the characteristics of the spectral and electrical properties. The schematic electrical setup of an ignition system is shown in Figure 1. A Variation of the capacitor (C_{Add}) directly in front of the suppression resistor (R_{SP}) shows the influence of parasitic or applied passive electrical components on the spark and, hence on the ignition behavior. Due to the positioning of the added capacitor, right in front of the suppression resistor, the capacity acts like C_{SP1} .

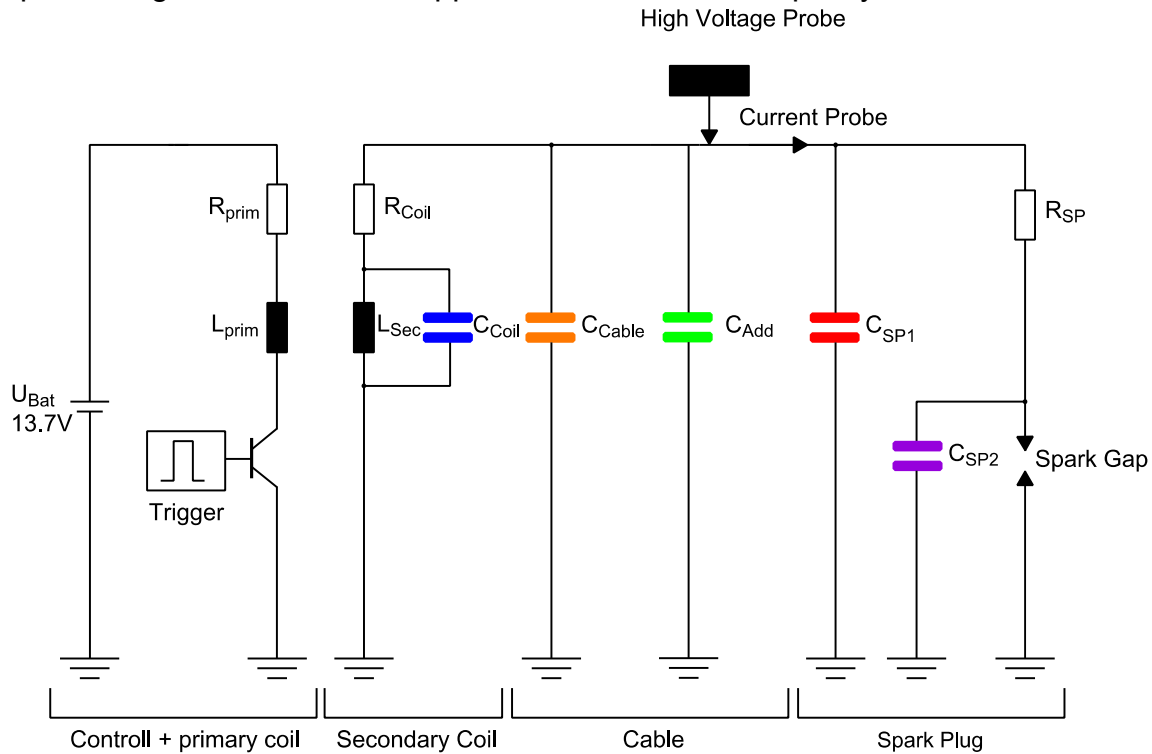


Figure 1: Schematic setup of an ignition system (derived from [2])

The ignition spark can be divided into the three discharge mechanisms breakdown, arc mode and glow mode [3]. These three phases source their energy from different parts of the ignition system. The different types of energy sources result in different types of discharge characteristics, here described as capacitive discharge and inductive discharge. Table 1 gives a rough overview of the distribution of the energy sources which supply the discharges.

Table 1: Overview of the type of discharges in a spark plug

Capacitive discharge		Inductive discharge	
Breakdown	Arc discharge		Glow discharge

The difference in the mechanism is based mainly on the physical processes for emitting electrons. Ahead of the breakdown an initial electron forms an avalanche whose number of charge carrier increases further. This context is explained by Equation (1) [4].

$$\gamma * (e^{a*d_{electrodes}} - 1) \geq 1 \quad (1)$$

with:

- γ : retroactivity coefficient
- a : ionization number
- $d_{electrodes}$: gap between electrodes

As soon as the critical number of electrons of about 10^6 to 10^8 is exceeded, the discharge mechanism changes from the avalanche to the streamer mechanism [5] [6]. Due to this change a streamer head is formed by electrons which possess a much higher mobility than the ions. Behind the streamer head, one finds the so-called streamer tail. At the boundary surface between these regimes recombination processes can lead to strong emitted rays. These rays can ionize the gas around the streamer head. This leads to a faster movement of the head, as compared to pure collision ionization. Due to by this faster movement, the breakdown happens one power of ten faster. The voltage directly ahead of the breakdown is at its maximum and can be score numbers of about 40kV. After formation of this first discharge channel the gap voltage decreases as described by Toepler's law [7]. The number of charge carriers passing the channel increases, which results in a higher conductivity in the gap.

The arc discharge is driven by the so-called thermionic field emission of electrons. This is a mixture of thermionic emission, where the electrons are emitted by the high temperature of the cathode, and field emission. Field emission provides electrons by tunneling through the cathode surface. In case of thermionic emission, the work function of the electrons is reduced by the so called Schottky effect [8]. This facilitates the electrons to tunnel through the material of the electrode surface. In most cases the necessary current density cannot be applied. The materials hit by a high current density channel were evaporated by the cathode from a narrow area at the front of the cathode [9]. This area has a range of about one mean free path. The electric field that increases by this accumulation of material allows tunnel processes through the cathode surface material. Electrode materials with a high melting point can evaporate only in a very small area of the cathode referred to as cathode spot. Another characteristic of the arc discharge are the very low values of voltage of only some umpteen of volts.

The glow mode is dominated by collision processes in the gas. It is relatively independent of the collision processes at the cathode. Electrons will be generated mainly by inelastic particle collisions in the gas. The field accelerates the electrons in the gas. If the kinetic energy is high enough, the electrons are able to ionize the atoms and molecules in the gas. Because of the ionization more electrons are released, which sustain the current flow. A high voltage of a few hundreds of volts makes the difference between the glow discharge and the arc mode.

2 Experimental Setup

2.1 Data Acquisition

The oscilloscope LeCroy Waverunner 6030 with a rise time of 4.67ns was used to determine the electrical indicators of current and voltage. A Tektronix P6015A positioned immediately in front of the terminal nut was used to quantify the high voltage of the secondary path. To gauge the current, a current probe Pearson Current Monitor Model 2877 with a rise time of 2ns and a critical frequency of 200MHz was used. Data recording was done at a sampling rate of 10MS/s. Calculation of the electrical energy was carried out using the following formula (2):

$$E_{elec} = \int_0^{t_{Spark}} (u(t) - R_{SP} * i(t)) * i(t) dt \quad (2)$$

with:

- E_{elec} : Electrical energy [J]
- t_{Spark} : Spark duration [s]
- $u(t)$: Voltage [V]
- $i(t)$: Current [A]
- R_{SP} : Suppression resistor [Ω]

For spectroscopy a Princeton Instruments Aceton SP-2500 with a PI-MAX 2 ICCD camera was used. A 600g/mm grating and a slit width of 20 μ m were used. Data acquisition was done using the program Winspec. With the aid of the spectrograph software, the camera and the ignition coil were triggered. The measurement procedure is described in the literature [10].

A Matlab based script allowed alignment of the data from the oscilloscope and the spectrograph. Assessment of the electrical and spectral data for each spark within the recorded timing window, based on the common trigger signal, was achieved using the same script.

2.2 Setup

Figure 2 shows the schematic setup for spectroscopic and electrical data acquisition. The spark plug and the ignition coil are arranged in a metal housing to protect the measurement devices from EMC. A spark plug with an electrode of nickel and a gap of 0.9mm was used. The resistance of the spark plug (R_{SP}) was 6.5k Ω . The coil used had ignition energy of 90mJ and an initial current of approx. 150mA.

2.1.1 Electrical Setup

From the PC controlling the spectrograph a trigger signal was sent to a function generator. Without significant delay, the latter transmitted another trigger signal to the ignition coil and the oscilloscope. The signal served as a trigger signal for the record and as the dwell time signal for the ignition coil. A 13,7V car battery was used as a DC power supply. From the ignition coil a high voltage ignition cable leads directly to the high-voltage probe. To this cable, the additional capacitors (C_{Add}) were attached. The probe the Pearson current monitor for determining the secondary current was placed

right behind the probe. Another ignition cable without resistance closes the high voltage circuit to the spark plug.

2.1.2 Spectroscopic Setup

The Programmable Timing Generator (PTG) was triggered by the PC of the spectrograph. The signal from the PTG was transferred to the CCD camera with a well-defined delay. This timing delay was not constant and changed its time lag. The delay was put together by the gate duration and the number of iterations passed through. For this reason the first $40\mu\text{s}$ had a gate window of $2\mu\text{s}$. From 40 to $400\mu\text{s}$ the window was $10\mu\text{s}$, and after that, the time window was $1000\mu\text{s}$. An exact description of the measurement method is given in [10]. Using the software Winspec the gate and the gain for the explorative area of wavelengths were defined. Transferred by an UV-objective the light of the ignition spark was guided to the $20\mu\text{m}$ slit of the spectrograph. The following wavelengths were used for evaluation: N_2 (337nm SPS), N_2^+ (391nm FNS) [11], Ni (341nm), N (500nm) and O (777nm) [12].

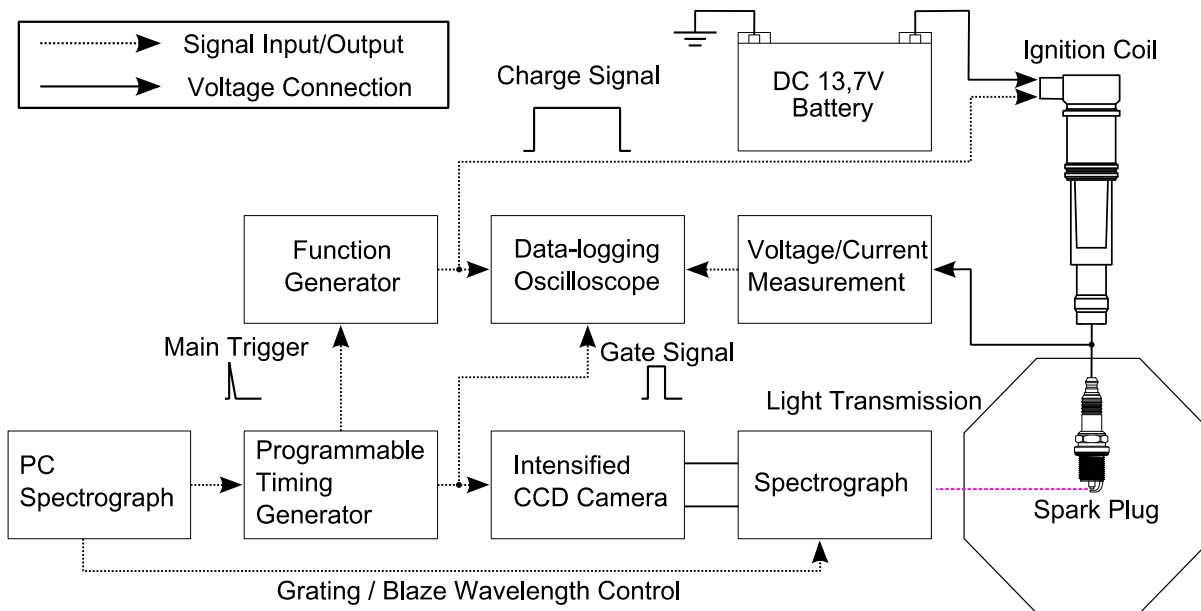


Figure 2: Schematic measurement setup [9]

3 Results

The results of spark emission spectroscopy and if the evacuation carried out afterwards are shown in Figure 3. On the left axis the distance from cathode to anode (in mm) is plotted. The right axis shows the cumulated electrical energy of arc and glow discharge. The measured intensities of the species named in Chapter 2.1.2 are colored. On the axis of abscissae, the spark duration is plotted. The breakdown was defined by an instant of zero. In the red box, the area described in the following section is emphasized (lower picture).

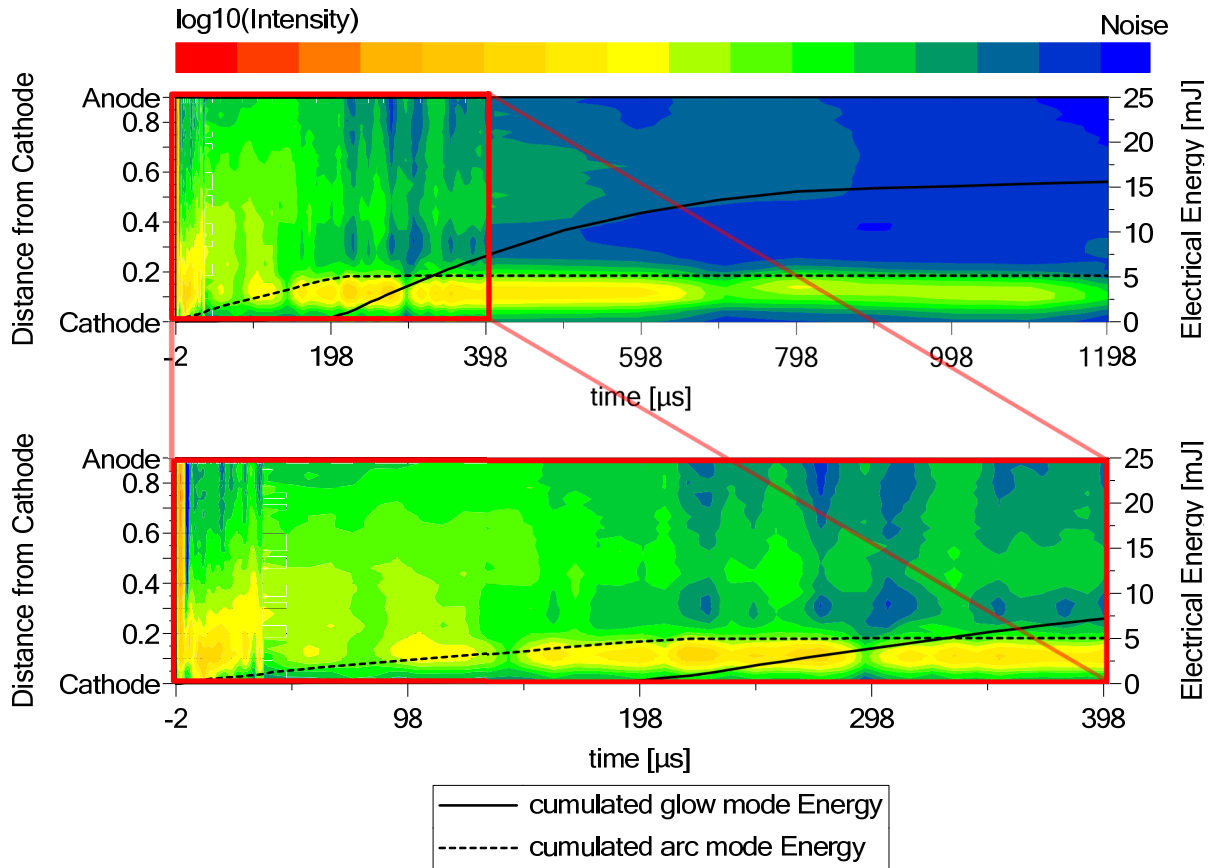


Figure 3: Intensity of N_2 at 337nm and electrical energy of arc and glow modes at 1 atm during a spark with a duration of 1200µs. Above: Entire spark. Below: First 400 µs of the spark.

The wavelengths of N_2 and N_2^+ were chosen because of the possibility to calculate the temperature with this two species. Also they were a good indicator for the energy transferred to the gas. Atomic nitrogen was chosen to get an indicator of the ability to dissociate the gas. To estimate the effects of the wear and to differentiate the arc and the glow mode the nickel line was observed. At last the atomic oxygen line was observed to get an indicator for the inflammability. In this work the dimension “Counts” will stand for the dimension of the measured intensity.

3.1 Ni at 341nm

The emission of nickel through the emission line at 341,48nm for different capacitors C_{Add} is shown in Figure 4. An important indication of arc discharge action is the enhanced emission of electrode materials as markers of the thermionic emission. During the breakdown only a small amount of nickel is traceable. During the variation of capacitors the radiation intensity is constantly lower than 2000 counts while the breakdown continues. Whenever the capacity mainly supplies arc discharge, the intensity increases rapidly more than tenfold. This effect grows with rising capacity. For the time the discharge is fed by the capacitors very high intensities of the cathode material nickel are measured. In fact there were some thousand counts of the radiation. With an increase in the capacitors the duration of the arc discharge and the duration of the height of the intensity remain at a very high level. When the current decreases, the emission gets weaker too. Nickel can be found primarily near to the cathode. By rising the capacity the radiation penetrates slightly deeper into the gap of the ignition spark. As soon as the discharge source changes to the inductance supply the qualities fall to approx. 4000-8000 counts. An independence of the penetration length in addition to the capacity can be observed. With the commencement of the glow mode, the intensity decreases to values below 2000 counts. The emission can be proven only in the immediate vicinity of about 150 μ m around the cathode.

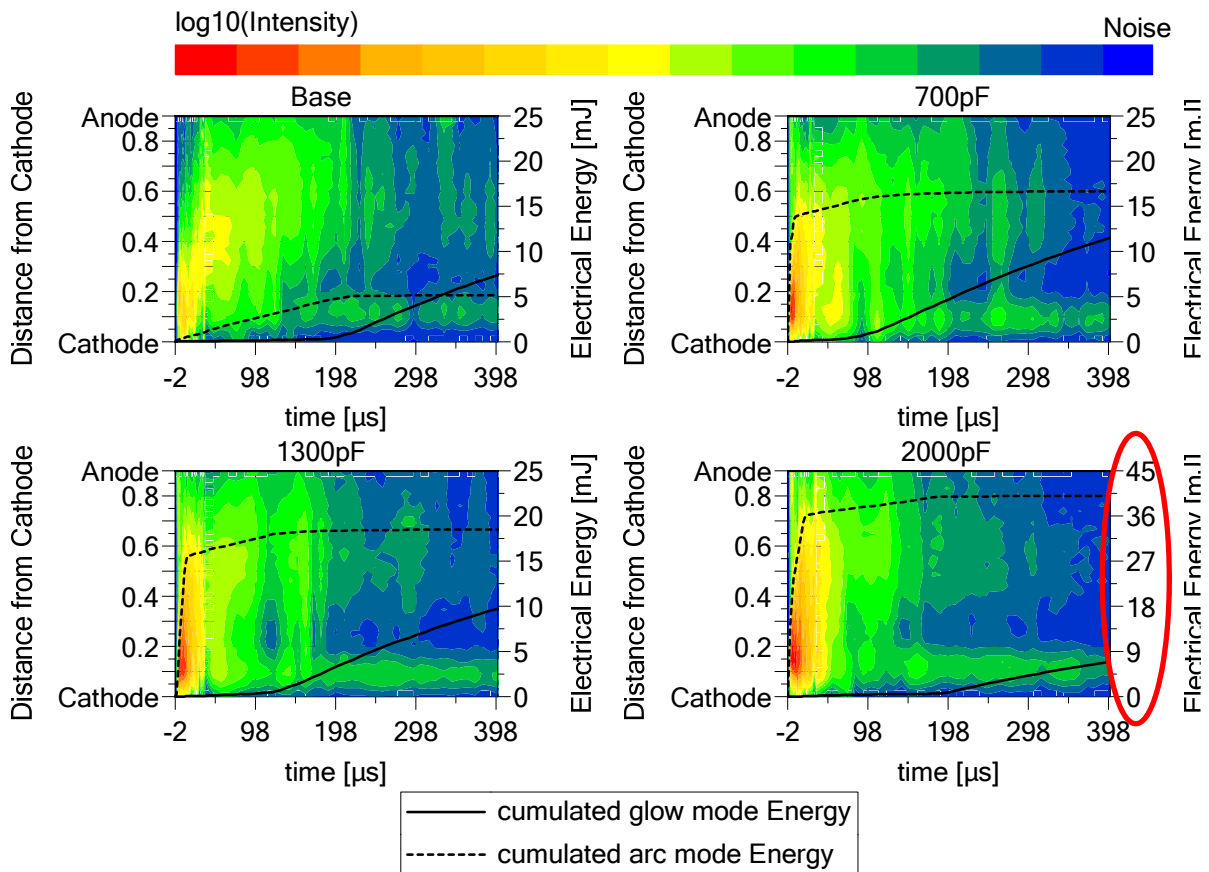


Figure 4: Variation in capacity from 0 to 2000pF for the emission of Ni at 341nm during the first 400 μ s.

3.2 N₂ at 337nm (Second Positive System)

A variation in capacitors leads directly to a higher intensity during the breakdown. The intensity increases from about 24000 to over 52000 (from 0pF to 2000pF). Figure 5 shows the increase in the duration of intensity (from about 2 to 40μs) and the intensity itself by accretive capacity during capacitive arc discharge. The intensity increases by about the multiplier of 2.7 when using an additional capacity of 2000pF. A nonlinear, slightly declining trend in the increase can be observed. While the capacitive discharge is active, the emission stays as a function of the capacitor increase. With increasing capacitor, the intensity that penetrates the gap, in direction of the anode, slightly increases. Subsequent to the arc discharge elicited by the capacitive discharge, an arc with energy supply from the inductance occurs. The duration of this phase reduces the increasing capacity from about 200-400μs to 50-100μs. During the period of the inductively supplied arc discharge the stimulation of N₂ is less intensive and percolates nearly the whole space in the gap. As soon as the glow discharge occurs an intensive luminous negative glow at a distance from 0 to 200μm from the cathode can be observed. Only in this range, an increased intensity can be found. In the remaining gap, one finds only a small fraction of the ray.

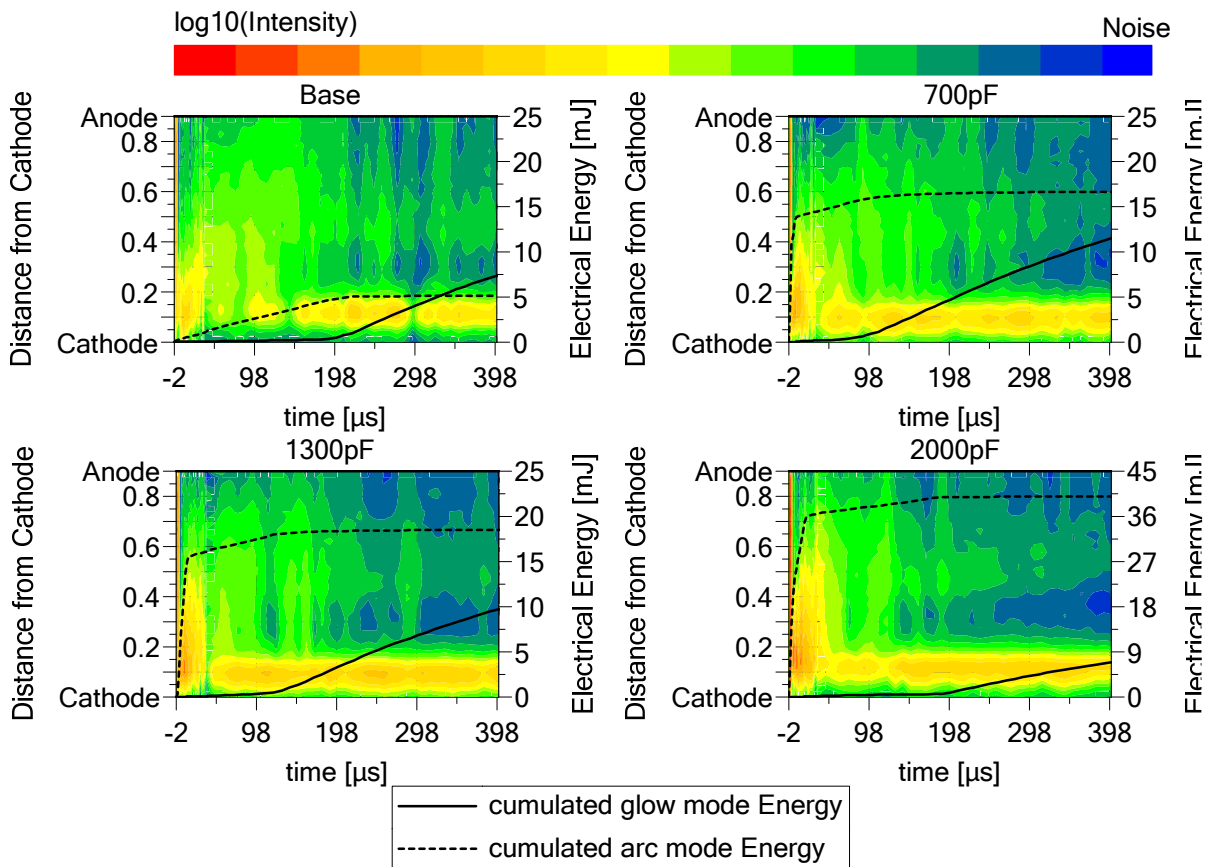


Figure 5: Variation in capacity from 0 to 2000pF for the emission of N₂ at 337nm during the first 400μs.

3.3 N₂⁺ at 391nm (First Negative System)

In Figure 6 the emission of nitrogen at 391nm is shown. During the whole time, the emission is restricted to the area of the cathode. During the breakdown, only a slight increase in emission can be observed. The intensity increases from about 1000 to 3000 counts with increasing capacitor. Over the course of the arc discharge supplied by the capacity the radiation intensity of nitrogen along the spark gap is very low. Only near by the cathode, a minor light emission can be perceived. The intensity in this area roughly reaches 2000 counts. For all capacitors the intensities are gaining the same values. For the inductively supplied arc mode, the same observations can be made. Analogous to the capacitive discharge, the intensity of radiation nearby the cathode is slightly exceeded. Also in this area, the intensity does not exceed the 2000 count level. The remaining area does not show any strong radiation. If transitions between arc and glow discharge occur, a strong increase in intensity can be observed. Immediately 5000-8000 counts can be detected. These values are measured up to a distance of about 200μm from the cathode. Beyond this section only a weak radiation is recorded.

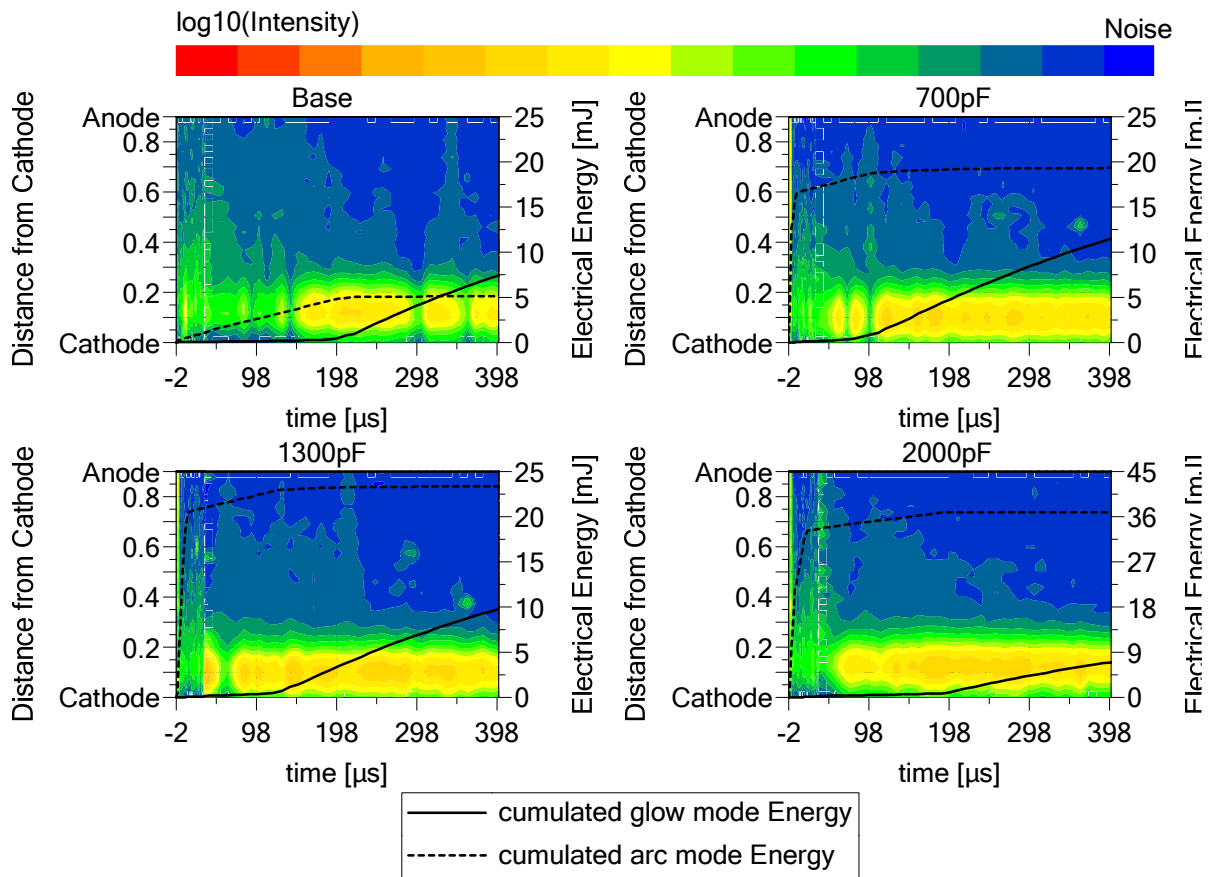


Figure 6: Variation in capacity from 0 to 2000pF for the emission of N₂ at 391nm during the first 400μs.

3.4 N at 500nm

The radiation intensity of atomic nitrogen can be found at a wavelength of 500nm. This trend is shown in Figure 7. During the breakdown the signal without an additional capacitor cannot be differentiated compared to the background noise. In the case of an added capacity of 2000pF the emission is above 8000 counts. Hence a high increase with respect to the signal without capacitor can be reached. With the start of the capacitive discharge, in the arc mode, an abrupt increase in intensity can be observed. By raising the capacity, the maximum value raises too. The penetration length of the radiation, however, is only little influenced. As long as the discharge is fed by the capacitors, the intensity is at a very high level. If the energy input occurs through the inductance the emission suddenly vanishes. No changes in this behavior can be observed whenever the transition between arc and glow discharge appears. Only a very facile radiation around the cathode is perceived. This radiation occupies a space of about 200 μm up to the cathode. Beyond this region, no radiation can be found.

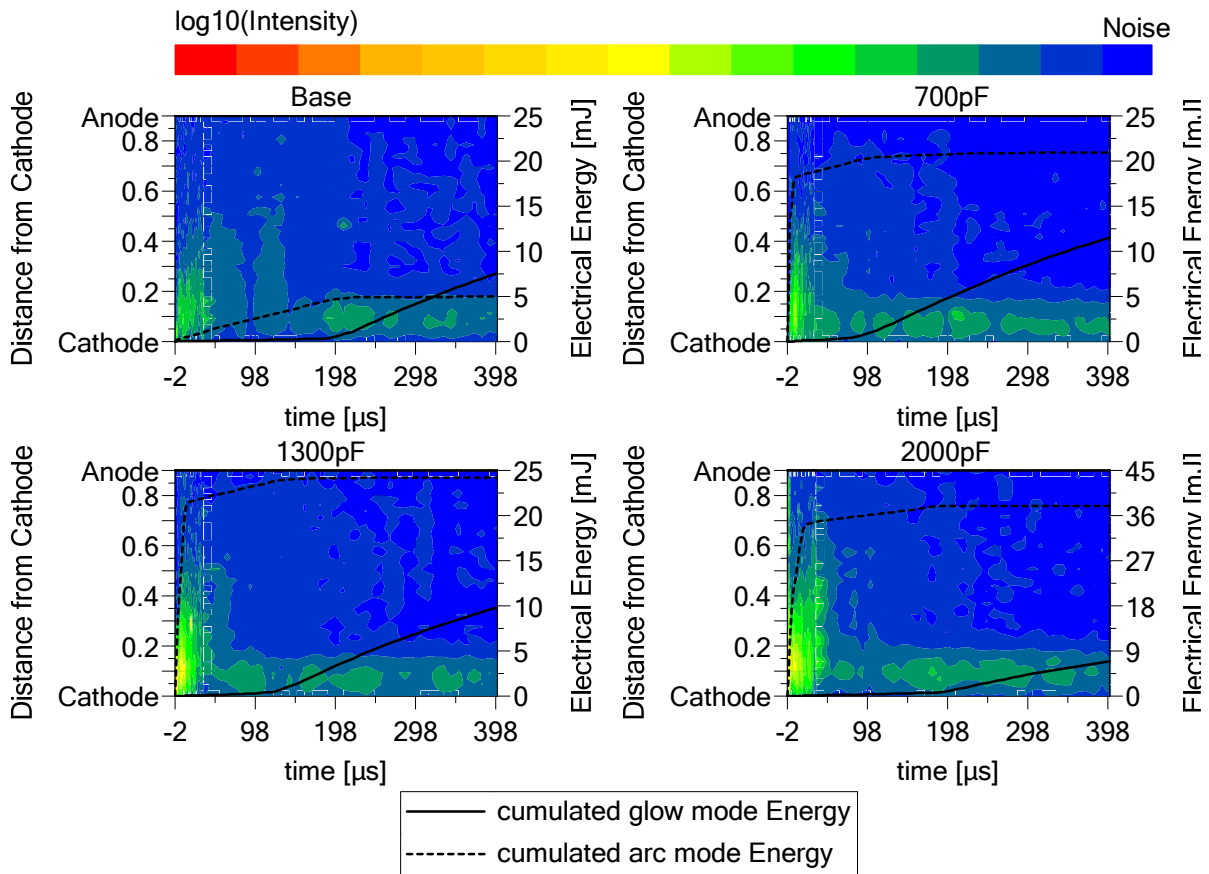


Figure 7: Variation in capacity from 0 to 2000pF for the emission of N at 500nm during the first 400 μs .

3.5 O at 777nm

Figure 8 shows the emission of triplet oxygen at a wavelength of 777nm. In the breakdown, a strong increase in intensity from 10000 to approx. 55000 counts is detected. This increase behaves nearly linear. From cathode to anode the radiation rises. The radiant intensity drops only shortly after the breakdown. The reduction in intensity with increasing capacity is an interesting and unexpected behavior. During the period of the capacitive duration of the arc discharge, the values of the radiation can be measured in a relatively low range of 1000 to 3000 counts. A decrease in the current results in a slightly grow of intensity. Also the extension in direction to the anode is slightly affected. A reduction of the current lowers the penetration lengths marginally. A strong increase in radiation can be found as soon as the energy source switches from the capacitors to the inductance. The maximum values are observed once there is no additional capacitor. These values can exceed 8000 counts. The penetration length remains nearly the same and is independent of the capacity. As an example, a penetration of the radiation at about 600 μ m from the cathode was measurable. When the transition from arc to glow discharge arises, the radiation gradually vanishes out of the space between the electrodes. Only around the cathode, up to a distance of 200 μ m, the radiant intensity remains like the previous similar level.

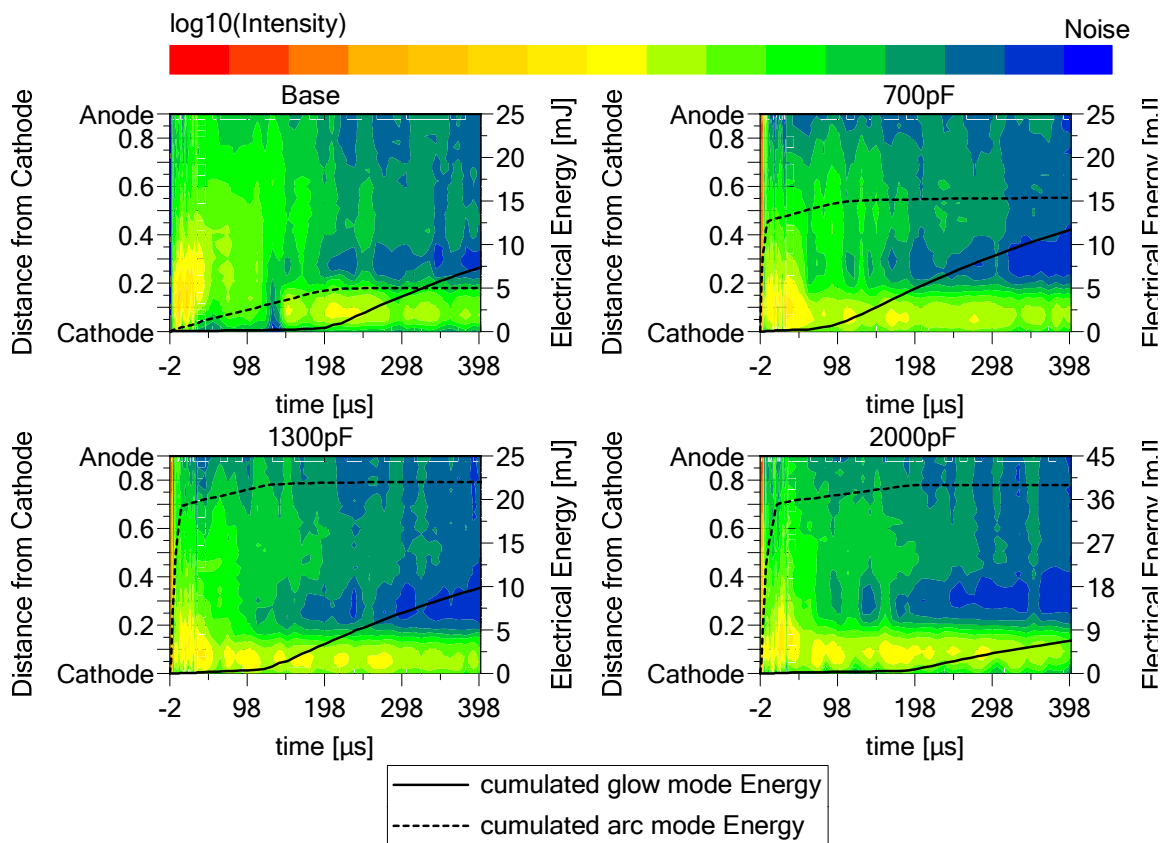


Figure 8: Variation in capacity from 0 to 2000pF for the emission of O at 777nm during the first 400 μ s.

4 Discussion

In this chapter the trends from chapter 3 were discussed and described with help of the plasma physical effects.

4.1 Ni at 341nm

The maximum voltage before the breakdown, on average amounts about 5kV. Compared to this, the static ignition voltage according to Paschen, amounts to 3.8kV for the given system. Thereof, a shock factor of 1.32 can be calculated. These high overvoltages in combination with the rough surface of the cathodes lead to the breakdown mechanism of streamer [13]. In consideration of the fact that this mechanism expires mostly in the gas, then interacting with the cathode, the nickel emission in the gas is very low.

Following the breakdown, the arc discharge, which gets its energy from the capacitors, occurs. Caused by the high sublimation temperatures of 3003K [14] for nickel and the low current of about 600mA, the maximum diameter of the cathode spots is 10 to 30 μ m [15] [2]. With the diameter as a measure for the plasma channel of the arc discharge, current densities between $8.5 \cdot 10^4$ und $7.6 \cdot 10^5$ A/cm² can be estimated. As described in [16], these densities lie between the transition from thermal and thermionic-field arc. An increased intensity and penetration length is caused directly by the higher density of electrode material in the gas.

After the period of capacitive discharge, the inductive time of the arc mode follows. As soon as the capacity is fully discharged, the current rapidly decreases to a lower level. A small step at the end of the capacitive discharge of about 150mA, without an additional capacity, to 100mA at 2000pF characterizes the end of the capacitive arc. Caused by the reduced current, the intensity and the duration of the inductive arc mode decrease. Up to current of approx. 100mA, a very stable arc can be observed. Certainly up to a current of 20mA, some rare transitions between arc and glow discharge are noticeable.

As the glow discharge sets in, the emission of nickel nearly disappears. Only close to the cathode is a small intensity of the cathode material measureable. This is caused by the low interaction of the glow discharge with the cathode. Mainly some atoms are released from the cathode by the effect of sputtering [17].

4.2 N₂ at 337nm

The capacity only affects the intensity of the breakdown. With its increase the maximum intensity grows from 24000 to 52000 counts. Furthermore, the intensity grows with the distance to the cathode. This leads to the conclusion, that, due to increased and faster energy storage, more electrons are available to excite the gas. The breakdown should be caused by a streamer. In the streamer head, considerable ionization and excitation occur. The streamer head is normally near to the anode. This could explain the growing intensity with increasing distance to the cathode.

During arc discharge from the capacitive source, the intensity and the penetration lengths have a high status. With decreasing current, both values are decreasing, too. Especially near to the cathode, the intensity is very high. This is caused by the electrons, which have a very high energy level after exiting the cathode surface. Because of this, the electrons are available for exciting the nitrogen at a very early stage. The

space between the electrodes is mostly occupied by the positive column of arc discharge. The emission of radiation in the positive column is decreases from the cathode in direction to the anode. Probably the electrons lose their energy during their travel through the positive column on account of, collision processes. This leads to a decrease in excited states in the case of constant gas density. With the higher duration of action and the slight increase in current, the penetration length increases too. It should be noted, that the excitation cross section of the second positive system (SPS) significantly increases with a rise in electron temperature [18]. Due to this, more molecules can be excited by electron collisions.

During the inductive arc mode a homogenous trend in radiation is measurable. Like in the case of the capacitive arc, the positive column occupies nearly the whole space between the two electrodes. The high energy of the electrons, when leaving the cathode surface leads to a high intensity directly in the vicinity of the cathode. With the increased capacity, the intensity at the cathode increases, too. An earlier transition from arc phase to glow discharge can be identified as the reason for this transition.

As the glow discharge sets in, the intensity nearby the cathode rises strongly. As long as a transition between the two modes is active, a high intensity at the cathode as well as an increased radiation of the positive column can be observed. When the glow discharge dominates, the intensity above a distance of 200 μm from the cathode decreases permanently. Because of the pressure (1 bar) and the electrode gap of 0.9mm, no positive column can be observed [19]. This area is referred to as Faraday dark space. Electrons could not accumulate the necessary energy to excite the molecules. This is caused by the high pressure and the small field which are leading to more collisions in the gas. The emission maximum is in a small distance from the cathode. At departure of the cathode the electrons have a very small energy of about 1eV [19]. With this energy, no atoms or molecules can be excited. With rising distance from the cathode, the electron temperature is increasing. This results in a higher excitation of the N_2 molecules.

4.3 N_2^+ at 391nm

The nitrogen radiation band of 391nm is a simply ionized nitrogen molecule. It has a very high ionization energy level of 15.58eV [20]. Like the SPS of nitrogen the FNS behaves similarly during the breakdown. With an increased capacity, the intensity grows. The maximum intensity is near to the anode. This can be explained analogously to the SPS. Caused by a higher energy storage, more electrons, from the capacitive storage are available in the breakdown. This leads to a higher excitation in the gas.

Only in direct proximity to the cathode, does a capacitive arc show an increased radiation of N_2^+ . With 150-200 μm , the penetration length is in a well-known-range. As the cathode surface is withdrawn, the energy of the electrons is the highest. According to this ionization of nitrogen near the cathode can be provided by the high electron temperature. With increasing distance from the cathode the energy of the electrons decreases by collisions in the gas. Therefore the discharge has not enough energy anymore to ionize the nitrogen.

The inductive arc behaves identically to the capacitive one and will therefore not be explained in this chapter.

Whenever the transition to the glow mode occurs, the first negative system (FNS) of nitrogen can be observed with a high intensive glow near the cathode. Caused by the high velocities of the electrons in this area, the degree of ionization and miscellaneous

excitation occurs [21]. In the remaining area between the electrodes, radiation is prevented in the Faraday dark space. The electrons have lost their whole energy in this zone almost completely and, hence, have to be accelerated again to effect further excitation.

4.4 N at 500nm

During breakdown, the intensity of atomic nitrogen strongly increases with the capacity. With increasing distance to the cathode, this intensity decays very fast. This behavior could be explained by a loss in electron temperature from cathode to anode. This causes a reduction in the dissociation probability of atomic nitrogen. Unfortunately, this explanation could not be confirmed during the preparation of this paper.

During arc discharge caused by the capacitor, a moderate intensity of radiation can be observed. With an increase in capacity and due to this, a capacitive arc with a longer duration and higher current, the atomic nitrogen density in the gas increases, too [22]. During this kind of arc, and, hence, with that a rapidly decreasing current, the emission of N at 500nm decreases, too. Regarding the mechanism of the arc discharge, when charge carriers mainly are triggered by the thermionic-field emission from the cathode, the change in penetration length can be explained as follows. With an increasing distance from the cathode, the thermal energy of the electrons is declining. This is caused by the process of inelastic collisions in the gas. After a certain distance, the electrons do not have enough energy anymore. The electrons are no longer available for dissociating the dinitrogen.

As inductive arc discharge sets in, the emission decreases rapidly. As long as this arc is active, nearly no emission can be measured. Probably, this effect depends on the reduced electron temperature and, hence, the lower chance of dissociating the molecule.

After transition to the glow discharge, the emission rises slightly in the zone of negative glow. This is assumed to be caused by the collection of ions and electrons with a higher energy level [19]. This glow is very low compared to the glow in case of capacitive arcs. The remaining spark gap is fully filled by the Faraday dark space with its very low electron energy.

4.5 O at 777nm

The transition from 5P to $^5S^0$ of OI (dissociated and excited directly from electron collisions [23]) revealed at a wavelength of 777nm. The dissociation and ionization of OI by electron collisions follows the following equation (3) [24]:



During breakdown, the intensity grows from the cathode to the anode. This indicates the formation of a streamer head. In this head, the ionization potential caused by electrode collisions and photoemission seems to dissociate and excite the oxygen.

During the capacitive arc discharge not much of the ionized oxygen at 777 nm can be measured. With an increase in capacity, the maximum intensity and the penetration length decrease. Unfortunately, the reason for this behavior could not be identified yet. A possible cause for this phenomenon could be a reduced excitation cross section. In

[25] and [26], the excitation cross section of the triplet oxygen at 777nm has its maximum at 16eV. Beyond this, this value rapidly decreases. For example, at an electron temperature of 26eV, the excitation cross section is halved compared to the maximum value. As an alternative, another energy level, e.g., the higher excitation level at 844 could be excited. Unfortunately, no alternative energy level was found. A potential reason for this is that the energy level is outside of the measurement range of the spectrograph.

A different trend is shown by the inductive arc discharge. Without an additional capacitor, a higher intensity and the penetration length, especially at the start of the discharge, can be observed. A final reason for this phenomenon could not be found. At this point, the same presumptions as for the capacitive arc, with the reduced excitation cross section, can be made. Only the higher radiation at the beginning of the discharge can be explained by the higher current of inductive compared to the capacitive arc. In direction to the anode, the intensity is constantly reducing. This is likely to be caused by the higher electron energy at this stage of the discharge.

As the glow discharge sets in, the emission can be located near to the cathode, where the negative glow takes place. The high densities of ions and electrons in this area result in a high radiation density of the species. The remaining dark area between the cathodes is the Faraday dark space where no emission can be found. In this area, the energy of ions and electrons is not high enough to dissociate, and with this reaction, to ionize the dioxygen to atomic oxygen.

5 Conclusion

An increase in capacity leads to very different results regarding the emission of the species N_2 , N_2^+ , N, Ni, and O from an ignition spark. Table 2 gives an overview of the effects, from a variation in C_{Add} to the emissions of the species, with the nomenclature: ++ strong increase, -- strong reduction, and 0 no effect to the considered parameters. In principle, a growth in the radiation intensity of N_2 , atomic nitrogen and especially nickel with an increase in the capacitor can be observed. All species, except for nickel, were increased in intensity by the capacity during breakdown. Particularly for the nickel emissions, the enhanced mechanism of arc discharge can be determined. Only a minor to no influence of the capacity on the remaining phases, the inductive arc, and the glow discharge was observed. This decrease is caused by the lesser disposal of energy from the inductive source. The first negative system of nitrogen at 391nm is largely unaffected by the capacity. During both arc discharges, the radiation of this system is only at a low level. The radiation increases as glow discharge starts. Only in the negative glow nearby the cathode, radiation is measurable. Considering the atomic oxygen triplet state at 777nm, the behavior of the radiation is different. With increasing capacity, the intensity, penetration length and duration of the radiation decrease. A final statement concerning thesis phenomena could not be made so far. A possible reason for these effects could be the change in the excitation cross section of this species.

Table 2: Impact of additional capacitors on the different phases of ignition sparks. (++) strong increase, (+) increase, (0) no influence, (-) decrease, (--) strong decrease.

Discharge Mode / Species	Characteristic Value	N ₂	N ₂ ⁺	N	Ni	O
Wavelengths [nm]		337	391	500	341	777
Breakdown	Intensity	++	+	+	0	+
	Penetration Length	0	0	0	0	0
	Duration	0	0	0	0	0
Capacitive Arc	Intensity	+	0	++	++	--
	Penetration Length	+	0	0	+	--
	Duration	++	0	++	++	--
Inductive Arc	Intensity	-	0	0	-	-
	Penetration Length	0	0	0	0	--
	Duration	-	-	0	-	-
Glow Discharge	Intensity	0	0	0	0	0
	Penetration Length	0	0	0	0	0
	Duration	-	-	0	-	-

Literature

- [1] J. Heywood, *Internal Combustion Engine Fundamentals*, New York: McGraw-Hill Inc., 1988.
- [2] J. Rager, *Funkenerosion an Zündkerzenelektroden*, Saarbrücken, 2006.
- [3] R. R. Maly und M. Vogel, „Initiation and Propagation of Flame Fronts in Lean CH₄-air Mixtures by the three modes of the ignition spark,“ in *Symposium (International) on Combustion*, 1979.
- [4] H. Reather, *Electron Avalanches and Breakdown in Gases*, London: Butterworths, 1964.
- [5] L. Loeb, *Basic Prozess of Gasous Electronics*, Berkley: University of California Press, 1960.
- [6] J. Meek and J. Craggs, *Electrical Breakdown of Gases*, New York: John Wiley & Sons, 1978.
- [7] M. Toepler, "Über Funkenspannungen," *Annalen der Physik*, vol. 324, pp. 191-209, 1906.
- [8] W. Schottky, "Über spontane Stromschwankungen in verschiedenen Elektrizitätsleitern," *Annalen der Physik*, vol. 362, pp. 541-567, 1918.
- [9] W. Ramberg, "Über den Mechanismus des elektrischen Lichtbogens," *Annalen der Physik*, vol. 12, pp. 319-352, 1932.
- [10] W. Kim, T. Michler, O. Toedter, T. Koch and C. Bae, "Time resolved emission spectroscopy for spark investigation," *International Conference on Ignition Systems for Gasoline Engines*, 6-7 12 2018.
- [11] F. R. Gilmore, R. R. Laher and P. J. Espy, "Franck-Condon Factors, r Centroids, Electronic Transition Moments, and Einstein Coefficients for Manx

- Nitrogen and Oxygen Band Systems," *Journal of Physical and Chemical Reference Data*, vol. 21, pp. 1005-1107, 1992.
- [12] A. Kramida and Y. Ralchenko, "NIST Atomic Spectra Database, NIST Standard Reference Database 78," 1999. [Online]. Available: <https://www.nist.gov/pml/atomic-spectra-database>. [Accessed 05 06 2018].
- [13] A. K uchler, *Hochspannungstechnik*, 3. ed., Schweinfurt: Springer, 2009, p. 178.
- [14] Y. Zhang, J. R. G. Evans and S. Yang, "Corrected Values for Boiling Points and Enthalpies of Vaporization of Elements in Handbooks," *J. Chem. Eng. Data*, vol. 56(2), pp. 328-337, 11 01 2011.
- [15] B. J uttner, "Cathode spots of electric arcs," *J. Phys.D: Appl. Phys.*, no. 34, pp. R103-R123, 21 08 2001.
- [16] A. Bauer, „Der Einfluss des individuellen Ionenfeldes auf die Thermo-Feldemission,“ *Beitr. Plasmaphys. (Beitr age aus der Plasmaphysik)*, Bd. 6, Nr. 4, pp. 281-298, 24 03 1966.
- [17] J. Coburn und E. Kay, „Positive-ion bombardment of substrates of rf diode glow discharge sputtering,“ *J. Appl. Phys.*, Bd. 43, p. 4965–4971, 1972.
- [18] H. H. Br omer und F. Spieweck, „Emission und Schwingungsverteilung der 1. neg. Gruppe und der 2. pos. Gruppe in einem,“ *Zeitschrift f ur Physik*, Bd. 184, Nr. 5, pp. 481-491, 1965.
- [19] A. Fridman and L. A. Kennedy, *Plasma Physics and Engineering*, 2 ed., CRC Press, 2011.
- [20] „National Insitute of Standards and Technology,“ [Online]. Available: <https://webbook.nist.gov/cgi/cbook.cgi?Formula=N2&Nolon=on&Units=SI&cTG=on&clE=on>. [Zugriff am 19 09 2018].
- [21] M. Lieberman und A. Lichtenberg, „Qualitative characteristics of glow discharges,“ in *Principles of Plasma Discharges and Material Processing*, New York, Wiley, 2005, p. 537.
- [22] E. Honanton, J. M. Palomares, M. Stein, X. Guo, R. Engeln, H. Nirsch und F. E. Kruis, „The transition from spark to arc discharge and its implications with respect to nanoparticle production,“ *J. Nanopart. Res.*, Nr. 15, 28 05 2013.
- [23] J. Jař ik, P. Macko, V. Martiřovitř, P. Luk a  und P. Veis, „Time Resolved Actinometric Study of Pulsed RF Oxygen Discharge,“ *Czechoslovak Journal of Physics*, Bd. 54, Nr. 6, pp. 661-676, 2004.
- [24] A. Kulikovsky, „Production of chemically acitve species in the air by a single positive streamer in a nonuniform field,“ *IEEE Transactions on Plasma Science*, Bd. 25, Nr. 3, pp. 439-446, 06 1997.
- [25] P. Julienne and J. Davis, "Cascade and radiation trapping effects on atmospheric atomic oxygen emission excited by electron impact," *J. Geophys. Res.*, vol. 81, no. 7, pp. 1397-1403, 01 03 1976.
- [26] Y. Itikawa und A. Ichimura, „Cross Sections for Collisions of Electrons and Photons with Atomic Oxygen,“ *J. Phys. and Chem. Ref. Data*, Bd. 19, Nr. 3, pp. 637-651, 3 05 1990.